Jurnal Teknologi

Full paper

Study of the Effect of Spacer Orientation and Shape in Membrane Feed Channel using CFD Modelling

H. C. Teoh*, S. O. Lai

Faculty of Engineering and Science, Universiti Tunku Abdul Rahman, Jalan Genting Kelang, Setapak, 53300, Kuala Lumpur, Malaysia

*Corresponding author: teohhc@utar.edu.my

Article history

Received :1 November 2013
Received in revised form :
1 June 2014
Accepted :30 June 2014

Graphical abstract

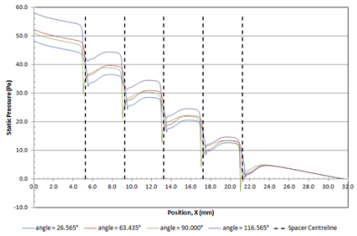

Abstract

Computational fluids dynamics (CFD) modelling has been carried out for a spacer-filled membrane channel using ANSYS FLUENT 14.0. The effect of spacer angles relative to the feed flow direction and different spacer shape combinations on velocity magnitude, wall shear stress, pressure drop and power number were investigated. From the results, spacer angle of 63.565° is the best orientation as it can generate the highest shear stress and reasonably lower power number compared to other spacer angles. Although the combinations of spacer shape did not significantly improve the average wall shear stress, it helped in reducing the pressure drop of the channel. The combination of triangular and circular spacers provided lower Power number, and hence lower energy consumption was required compared to pure triangular spacer. The current results indicated that a combination of triangular and circular spacers can be employed to offer better saving in energy consumption.

Keywords: Computational fluids dynamics (CFD); spacer geometry; shear stress; pressure drop; power number

1.0 INTRODUCTION

Recent years, membrane processes have played an increasingly important role in industrial separation. It has been established as a primary technology for ensuring the purity and efficiency of water treatment. There are four primary configurations for membrane processes, i.e. spiral wound, plate and frame, hollow fibre and tubular. For water treatment applications, spiral wound membranes are commonly used because of their high packing density and low cost. In this module, the membrane layers are wound around a central tube and the adjacent membrane leaves are kept apart by feed spacers to provide a channel for the feed. The feed spacers on one hand disrupt the flow and destabilise the boundary layer, resulting in increased mixing and mass transfer rates, but on the other hand, they increase the pressure drop and create stagnation zones where concentration polarisation may be enhanced. Thus, spacer designs which can promote mass transfer, while minimising energy losses and fouling will result in economic improvements for a membrane process.

Computational fluid dynamics (CFD) is mainly used to model the flow and concentration polarisation in a membrane system or narrow channel. The parameters that affect a membrane process are usually non-linear and are suitable to be solved using numerical simulation such as CFD approach. The attraction of this approach is that it is possible to observe the effects of different parameters on the system performance. CFD studies have also been carried out to model the flow pattern of different spacer geometries in the membrane modules [1, 2].

It is theoretically feasible to use the basic transport governing equations for laminar as well as turbulent flows. However, since most of the membrane processes work under laminar conditions, many authors are interested in the simulation of these conditions [1, 3, 4, 5]. Work by Fletcher and Wiley [6] reported that neither gravity nor density variation had a significant effect on the CFD solutions obtained for flow in a narrow channels. Thus, most published literature for membrane flow using CFD modelling has employed constant density and neglected the effect of gravity. The fluid is also typically assumed to be Newtonian with constant physical properties and the flow is assumed to be isothermal.

Numerous CFD works have been carried out in two dimensions (2D) due to its simplicity and smaller computational demands. These 2D CFD studies provided insight into the effect of geometry for different spacers, indicating that careful selection of spacer thickness, spacing and shape is crucial for minimising concentration polarisation. Shakaib *et al.* [7] investigated the effect of spacer geometry on mass transfer and fluid dynamics in a spacer-filled channel. Their CFD simulations revealed significant influence of spacer geometry on mass transfer coefficients and wall shear stress. Apart from the spacer geometry such as filament spacing and thickness in the feed channel, the performance of a membrane module is also strongly influenced by the shape of the spacers. Ranade and

Kumar [8] used a CFD model to evaluate the performance of different spacer shapes to investigate the effects of spacer shape and the resulting fluids dynamics. The models were also extended to simulate flow in curvilinear channels, which is useful in understanding the fluid behaviour in spiral wound modules. Their result showed that the fluid dynamics of spacer-filled flat and curved channels was not significantly different. Results obtained with flat channels could therefore be used to estimate the performances of spiral wound modules.

A study by Subramani *et al.* [9] found that on average, feed spacers reduced the extent of concentration polarisation due to the enhanced wall shear stress. However, their findings also proved that the stagnant regions in front and behind some spacer filaments would lead to enhanced concentration polarisation. This confirms the need to determine an optimal spacer geometry that can enhance wall shear rates and at the same time reduce stagnant zones inside a membrane channel. The spacers inside a membrane channel will also increase the pressure drop over the channel. An analysis by Da Costa *et al.* [10] on the processing costs in spacer-filled channels demonstrated that there were possibilities to optimise the spacers in order to reduce energy losses.

CFD simulation is an attractive approach because it not only yields a better understanding of the processes involved in membrane fouling, but also minimises the number of experiments needed to explore a wide range of parameters. Experimental studies may only provide qualitative information on fouling phenomena and concentration polarisation, whereas CFD simulation offers the possibility to model many situations with minimal cost. The adoption of CFD over the recent years has increased, as experimentations usually involve higher costs and more time consumption. With the enhancement of computing power and efficiency, CFD has become an effective tool to achieve the objective of a better design and more cost effective for spiral wound membrane process.

2.0 CFD SIMULATION

2.1 Spacer Orientations and Geometries

The computational domain comprised of a rectangular channel 31.5 mm long and 1 mm high. The channel was filled with 5 spacers of different orientations and shapes as shown in Figures 1 and 2. Each spacer had the same base length and height of 0.5 mm. The first spacer was located 5 mm from the channel inlet and the last spacer was located 10 mm from the channel outlet to eliminate the effect of entrance and exit on the fluid flows[11]. The distance between each spacer was fixed to 4 mm. Triangular spacer currently might not be available commercially, but the work from Ahmad *et al.* [11] showed that these spacers could offer better concentration polarisation reduction with minimal energy loss, and thus it is crucial to investigate the effectiveness of the triangle spacer on controlling pressure drop and minimising concentration polarisation. Since different spacer shapes will have different effects on the velocity profile, wall shear stress and pressure drop, combinations of different spacer shape (Figure 2) were incorporated into the channel in this study to take advantage of the different effects offered by different spacer shapes.

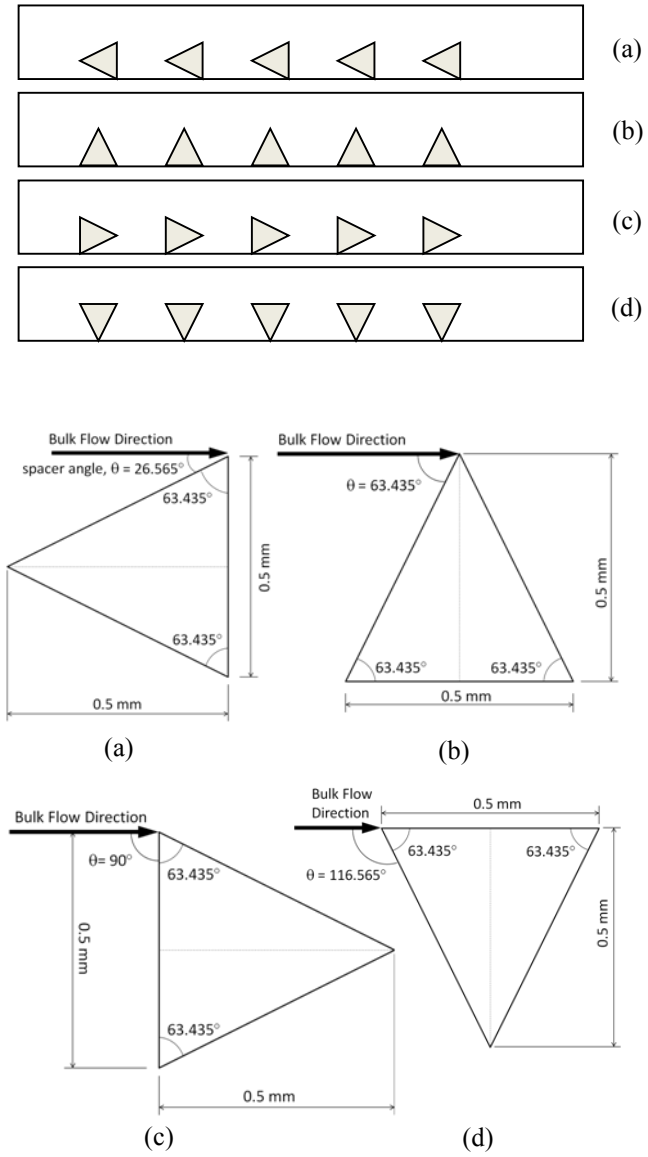

Figure 1 The simulation domain and orientations of triangular spacers with different spacer angle θ. (a) θ = 26.565°, (b) θ = 63.435°, (c) θ = 90.000°, (d) θ = 116.565°

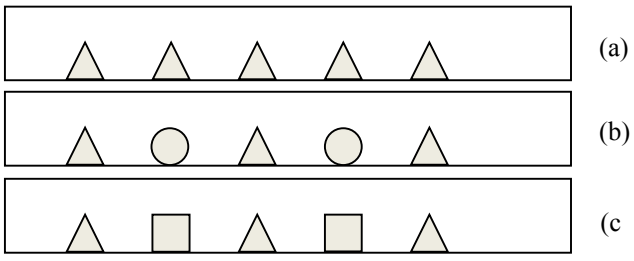

Figure 2 The simulation domain and combinations of different spacer shapes. (a) pure triangular shape, (b) combination of triangular and circular, (c) combination of triangular and square

2.2 Simulation Assumptions and Procedures

In the present study, the fluid used was water with constant density of 998.2 kg/m^3 and viscosity of 0.001003 kg/m-s. The channel's Reynolds number (Re_{ch}) was kept low at 100 for all cases [12] to enable the use of laminar flow model to simulate the flow through the computational domain. The spacer surfaces were defined as wall in the simulation. Since for most membrane processes the inlet velocity is 3–4 times higher compared to the permeation velocity, it is satisfactory to assume impermeable walls for the membrane layers with no-slip conditions [12].

The governing equations as expressed in Equation (1)–(3) were used to solve the steady, two dimensional and laminar fluid flow in the membrane channel.

Continuity equation:

$$\frac{\partial(\rho u)}{\partial x}+\frac{\partial(\rho v)}{\partial y}=0 \tag{1}$$

Navier-Stokes equation in *x*-direction:

$$u\frac{\partial(\rho u)}{\partial x}+v\frac{\partial(\rho u)}{\partial y}=-\frac{\partial P}{\partial x}+\frac{\partial}{\partial x}\left(\mu\frac{\partial u}{\partial x}\right)+\frac{\partial}{\partial y}\left(\mu\frac{\partial u}{\partial y}\right) \tag{2}$$

Navier-Stokes equation in *y*-direction:

$$u\frac{\partial(\rho v)}{\partial x}+v\frac{\partial(\rho v)}{\partial y}=-\frac{\partial P}{\partial y}+\frac{\partial}{\partial x}\left(\mu\frac{\partial v}{\partial x}\right)+\frac{\partial}{\partial y}\left(\mu\frac{\partial v}{\partial y}\right) \tag{3}$$

The channel Reynolds number introduced by Schock and Miquel [13] was adopted in this study and is given by:

$$\mathrm{Re}_{ch}=\frac{u_{av}d_h}{\nu} \tag{4}$$

whereby d_h is the hydraulic diameter for a spacer-filled channel given by:

$$d_h=\frac{4\varepsilon}{\frac{2}{h_{ch}}+(1-\varepsilon)S_{v,sp}} \tag{5}$$

ε is the porosity of the spacer-filled channel given by Eq. (6), h_{ch} is the channel height and $S_{v,sp}$ is the specific surface of the spacer given by Eq. (7).

$$\varepsilon=1-\frac{\text{spacer volume}}{\text{total volume}} \tag{6}$$

$$S_{v,sp}=\frac{\text{wetted surface of spacer}}{\text{volume of spacer}} \tag{7}$$

Power number (*Pn*), which represents the cross-flow power consumption, can be used to compare the energy consumption of different spacer configurations as defined by Li *et al.* [14]. The power number (*Pn*) can be calculated using pressure drop results obtained from simulations and the following equations.

$$Pn=SPC\frac{\rho^2h_{ch}^4}{\mu^3} \tag{8}$$

whereby *SPC* is the specific power consumption given by:

$$SPC=\frac{u_{av}\Delta P}{L_c} \tag{9}$$

In the above equations, ΔP is the pressure drop across the channel, L_c is the channel length, u_{av} is the average velocity, μ is the dynamic viscosity and ρ is the density.

To ensure mesh independence, initial simulations were carried out with finer and finer grid size until further increase in the mesh size did not produce significant difference (< 0.5%) in the results for the average velocity, shear stress and pressure drop. Figure 3 shows the simulation results for five different mesh sizes (20 k–60 k) with triangular spacers. The differences in average velocity, shear stress and pressure drop for 60 k and 50 k mesh size were less than 0.5% compared to those for 40 k mesh size. Thus, 40 k cells were sufficient to mesh the system, and eventually the computational time could be saved.

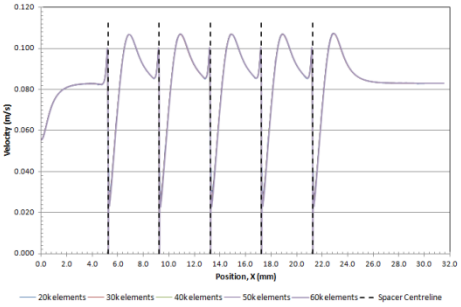

(a)

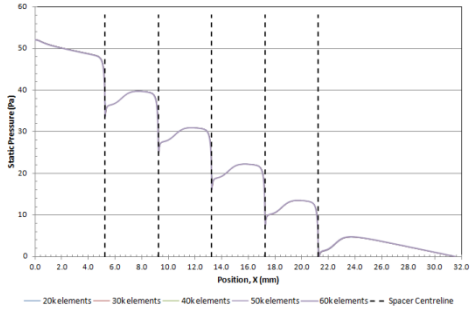

(b) (5)

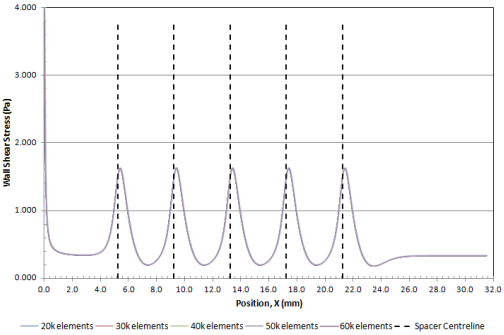

(c) (6) (7)

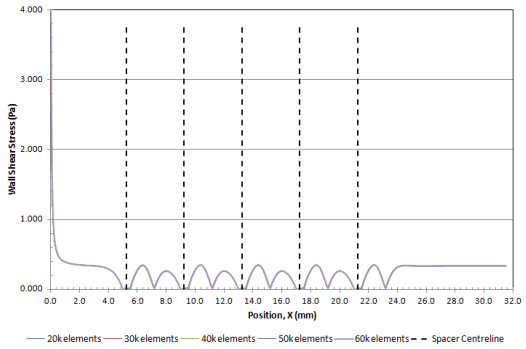

(d)

Figure 3 Mesh comparison for triangular spacers for five different mesh elements. (a) Velocity magnitude at y = 0.50 mm, (b) static pressure, (c) wall shear stress at top wall, (d) wall shear stress at bottom wall

ANSYS FLUENT 14.0 was used to simulate the fluid flow in the narrow channel, in which the governing equations were solved using a control-volume-based technique. The pressure and velocity were coupled and solved by Semi-Implicit Method for Pressure Linked Equation Consistent (SIMPLEC) algorithm, whereas Quadratic Upstream Interpolation for Convective Kinetics (QUICK) was used for the discretisation of momentum equations. Convergence criteria for the residuals of continuity and momentum equations were set to 1×10^{-7} for steady-state simulation.

3.0 RESULTS AND DISCUSSION

Two case studies were carried out to investigate the effect of feed spacer geometry on velocity magnitude, shear stress, pressure drop and power number by changing the spacer angle relative to the feed flow direction, and the spacer shape combinations.

3.1 Effect of Triangular Spacer Angle Relative to Bulk Flow Direction

The effect of changing the spacer angle θ relative to the bulk flow direction was investigated (Figure 1). Figure 4 depicts the velocity profiles for different spacer angles at the top, middle and bottom walls. The increment or reduction in the velocity profiles indicated that the presence of spacer played a role as a turbulent promoter or as an obstacle to form either highest velocity at the top wall or stagnant flow at the lower wall. High velocity region could be observed near the top wall above the spacers and reached a minimum value between two consecutive spacers. This indicated the generation of local high velocity field which could help in increasing the scouring force on the wall. At the middle of the spacer-filled channel as shown in Figure 4(b), the velocity reached the maximum value between two consecutive spacers. The velocity reduced as it went along the channel and just before the flow reached the subsequent spacer which acted as a turbulent promoter, the velocity increased again before it reduced to zero at the spacer. At the bottom wall, as shown in Figure 4(c), there were two peaks of high velocity between two consecutive spacers, and the minimum value occurred at the centre of the two consecutive spacers.

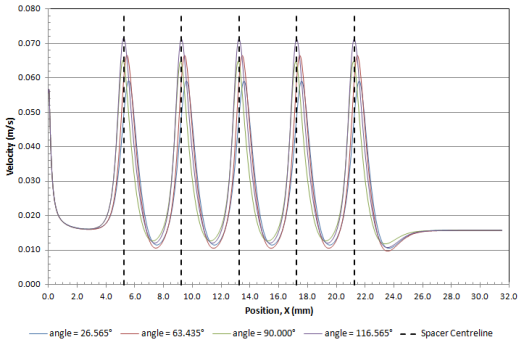

(a)

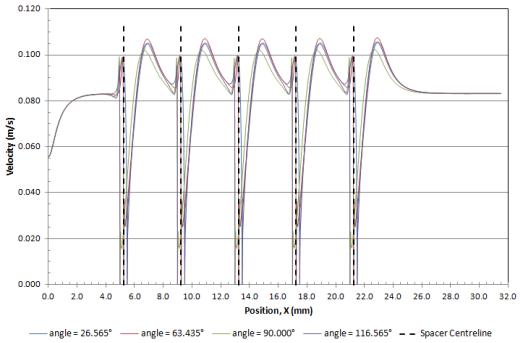

(b)

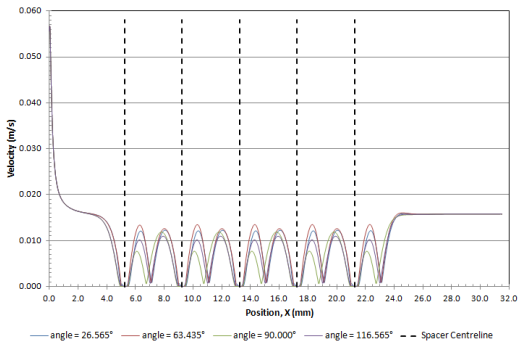

(c)

Figure 4 Velocity profiles for four different spacer angles along the x-axis. (a) near top wall (y = 0.95 mm), (b) middle channel (y = 0.50 mm), (c) near bottom wall (y = 0.05 mm)

Referring to Figure 4, the velocity magnitude was the highest for spacer angle of 116.565° followed by spacer angle of 63.435° at the top channel wall. The highest velocity was generated by spacer angle of 116.565° at the top wall due to its geometry, whereby the base of its triangle that was parallel to the top wall created a narrow space that accelerated the flow that passed through it. The rapid and sudden reduction and expansion in volume caused an increase in the fluid velocity field. For the middle and bottom wall, the orientation with a spacer angle of 63.435° tended to generate higher velocity magnitude compared to the other orientations. This could be attributed to the geometry of this spacer angle, whereby its slanted side provided a smooth and unobstructed path to the

bottom wall after the spacers. The pointed tip of spacer angle of 63.435° also helped in dragging and accelerating the fluid flow. For the spacer angle of 90°, the velocity was the lowest right after the spacer due to the stagnant zone below the spacer.

Figure 5(a) and (b) showed the variations of shear stress along the *x*-axis on the top and bottom walls, respectively. Generally, higher wall shear stress implies higher shearing effect on the membrane wall which subsequently can reduce the formation of concentration polarisation. When the fluid flowed through the narrow space above the spacer, it was accelerated and thus the highest value for shear stress was observed right above the spacer for the top wall and dropped to the lowest value at the centre of two consecutive spacers. For the bottom wall, as the shear stress distribution was mainly dependent on the velocity field, it reached the highest value just after the spacer, dropped to the lowest value at the centre of two consecutive spacers, rose again and dropped to zero at the spacer. This result is different from those obtained by Saeed *et al.* [12] which simulated the narrow channel with circular spacers. Their results concluded that the shear stress for the bottom wall reached a maximum value close to the centre of two consecutive spacers. This discrepancy was possibly due to the nature of triangular spacer whereby its slanted side provided an unobstructed path to the bottom wall after the spacer, but the effect wore off after a certain distance and thus the shear stress value reached minimum at the centre of two consecutive spacers. When the flow reached the subsequent spacer, the spacer acts as a turbulent promoter, and hence the shear stress increased again.

Comparing the effect of different spacer angles, Figure 5(a) demonstrated that the spacer angle of 116.565° generated the highest wall shear stress at the top channel wall, while spacer angle of 26.565° generated the lowest. The narrow space above the 116.565° spacer accelerated the flow that passed through it and this generated a high wall shear stress on the top wall. For the bottom wall, the spacer angle of 63.435° tended to generate higher wall shear stress compared to the other spacer angles. This was probably due to the geometry of this spacer angle whereby its slanted side provided a smooth and unobstructed path to the bottom wall after the spacers. The spacer angle of 90° generated the lowest shear stress right after the spacer due to the stagnant zone below the spacer. The shear stress distribution matched the velocity flow distributions as shown in Figure 4.

In a spacer-filled channel, pressure drop is an unavoidable phenomenon and the extent of pressure drop depends on the geometry of the obstructions or spacers in the channel. Figure 6 shows the static pressure for the four different spacer angles. It could be observed that the pressure decreased rapidly near the spacer area. Based on the result obtained, the spacer angle of 116.565° produced the highest pressure drop, whereas the spacer angle of 26.565° produced the least. It could be explained that the former spacer angle provided smaller gap for the fluid to flow through than the latter which directly increased the pressure drop in the channel. The fluid was forced to compress to fill the smaller gap at the top region of the spacer and subsequently expanded to fully fill the whole channel with 1 mm height. For the spacer angle of 26.565°, the fluid followed the ascending edge of the triangular spacer, which indicated a slow reduction in the gap. This slow process resulted in lower pressure drop along the channel. Figure 7 presents the Power numbers for the four different spacer angles, which were in accordance with the static pressure results, whereby the spacer angle of 116.565° had the maximum power consumption and the spacer angle of 26.565° had the minimum.

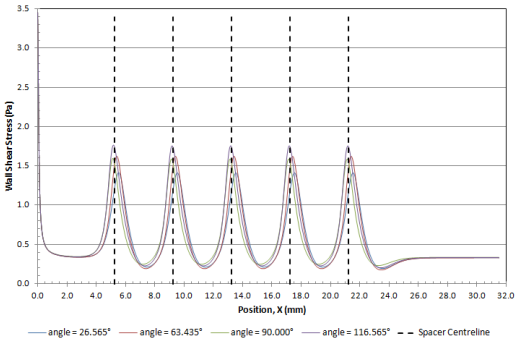

(a)

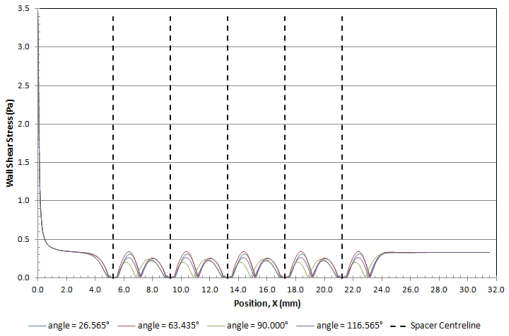

(b)

Figure 5 Wall shear stresses for four different spacer angles along the *x*-axis on (a) top wall (y = 1 mm), (b) bottom wall (y = 0 mm)

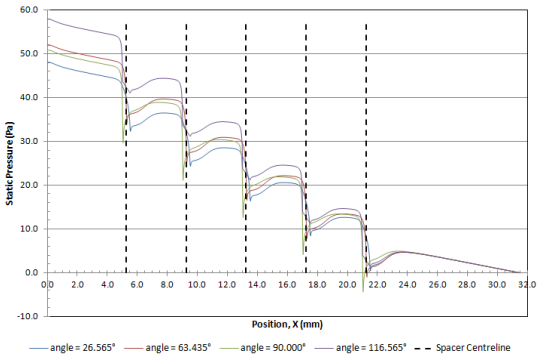

Figure 6 Static pressures for four different spacer angles along the *x*-axis

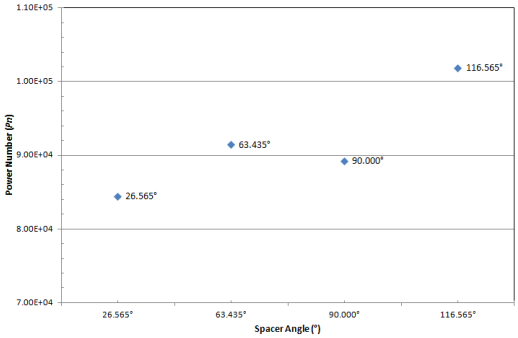

Figure 7 Power numbers (*Pn*) for four different spacer angles

3.2 Effect of Spacer Shape

Based on the work of Ahmad *et al.* [11], different spacer shapes exhibited different effects on the velocity profile, concentration polarisation minimisation and pressure drop. Triangular and square spacers were found to be able to generate higher wall shear stress and offer better concentration polarisation reduction at low flow rate, whereas at higher flow rate, circular spacer could result in lower pressure drop and hence lower energy loss. In this study, combinations of different spacer shapes (Figure 2) were incorporated into a channel to take advantage of the different effects offered by different spacer shapes. The results for velocity magnitudes and wall shear stress are presented in Figure 8 and 9, respectively. It could be noticed that different spacer shapes yielded the same evolution trends, in which the triangular spacer generated the highest velocity and wall shear stress followed by square shape and circular shape at the bottom wall and middle of the channel. The triangular spacer had a pointed tip which dragged the fluids severely and created high velocity at the middle of the channel, where the tip was located. The circular shape spacer created the minimum wall shear stress because the drag force generated by the rounded surface was insufficient to promote high velocity magnitude. At the top wall, the square shape spacer generated the highest velocity and wall shear stress. This was due to the geometry of the square spacer which provided a narrow space above the spacer and forced the flow to be accelerated, and thus produced higher wall shear stress on the top wall. These observations agreed with the work done by Ahmad *et al.* [11]. On average, the pure triangular spacers still provided the highest wall shear stress followed by combination of triangular/square and triangular/circular spacers. The combinations of spacer shape did not actually offer any improvement on the average wall shear stress.

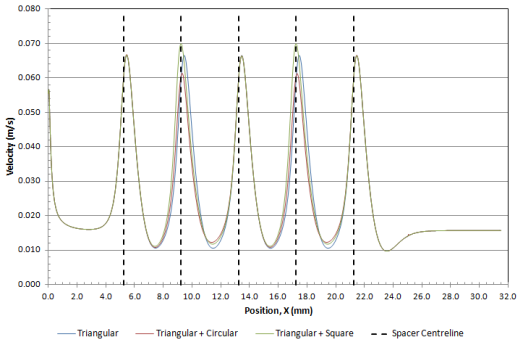

(a)

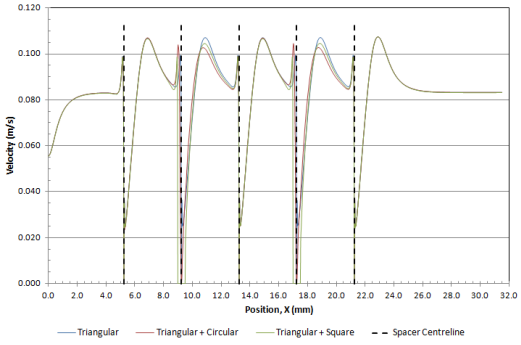

(b)

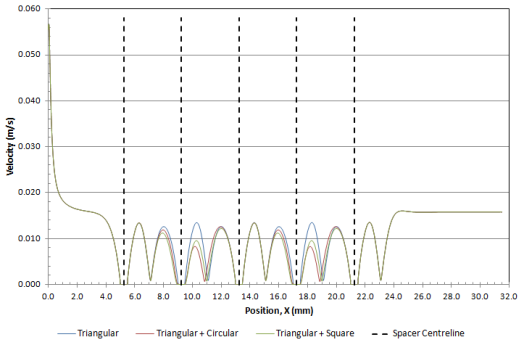

(c)

Figure 8 Velocity profiles for different combinations of spacer shapes along the *x*-axis. (a) near top wall (y = 0.95 mm), (b) middle channel (y = 0.50 mm), (c) near bottom wall (y = 0.05 mm)

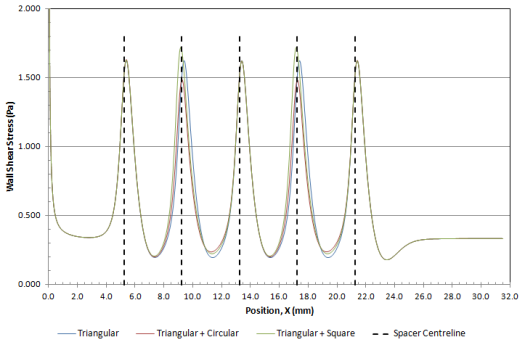

(a)

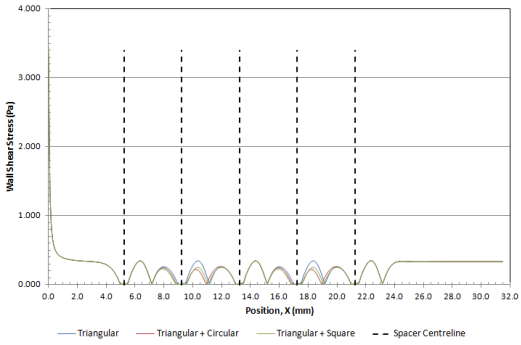

(b)

Figure 9 Wall shear stresses for different combinations of spacer shapes along the *x*-axis on (a) top wall (y = 1 mm), (b) bottom wall (y = 0 mm)

However, the combinations of spacer shape did offer some improvement in reducing the pressure drop of the channel, as can be seen in Figure 10 and Figure 11. The combination of triangular and circular spacers provided lower Power number and hence lower energy consumption was needed compared to pure triangular spacer. The flow distributions obtained were in fair accordance with the results available in literature [11, 15] whereby the circular spacer generated lower pressure drop compared to other spacer shapes. Combination of triangular and square spacers had the highest pressure drop and in turn the highest Power number since the fluid was forced to accelerate as a result of the narrow space availability above the spacer. The reduction in volume for the fluid to flow would directly increase

the pressure drop of the channel. It could also be observed that the pressure decreased rapidly near the spacer area.

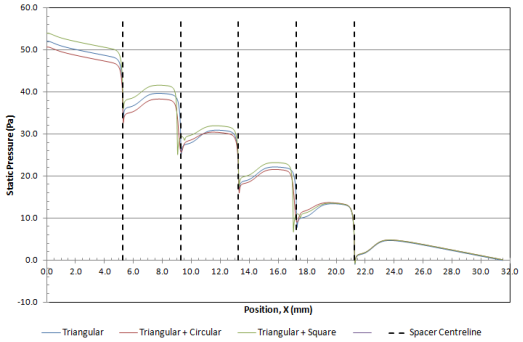

Figure 10 Static pressures for different combinations of spacer shapes along the *x*-axis

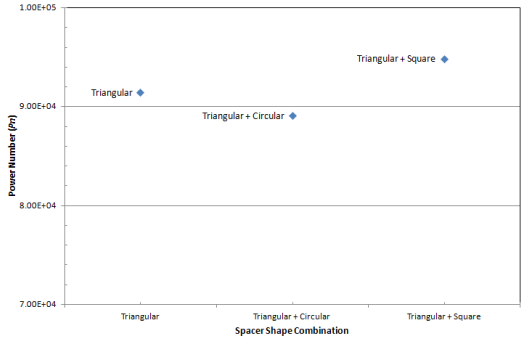

Figure 11 Power numbers (*Pn*) for different combinations of spacer shapes

4.0 CONCLUSION

The effect of spacer angles relative to the feed flow direction and different spacer shape combinations on velocity magnitude, wall shear stress, pressure drop and power number were investigated in this study. The spacer angle of 63.565° was the best orientation to be used in a narrow channel as it could generate the highest shear stress and reasonably lower power number compared to other spacer angles. Although the combinations of spacer shape did not offer any improvement on the average wall shear stress, it did help in reducing the pressure drop of the channel. The combination of triangular and circular spacers provided lower Power number, and hence lower energy consumption was required compared to the pure triangular spacer. Thus, a combination of triangular spacer with spacer angle of 63.565° and circular spacers can be employed to offer better saving in energy consumption.

References

[1] Bouchard, C., Carreau, P., Matsuura, T., Sourirajan, S. 1994. Modelling of Ultrafiltration Predictions of Concentration Polarization Effects. *J Membr. Sci.* 97: 215–229.
[2] Rahimi, M., Madaeni, S., Abolhasani, M., Alsairafi, A. 2009. CFD and Experimental Studies of Fouling of a Microfiltration Membrane. *Chem. Eng. Process*. 48: 1405–1413.
[3] De Pinho, M.N., Semião, V., Geraldes, V. 2002. Integrated Modeling of Transport Processes in Fluid/Nanofiltration Membrane Systems. *J Membr. Sci*. 206: 189–200.
[4] Geraldes, V., Semiao, V., De Pinho, M.N. 2001. Flow and Mass Transfer Modelling of Nanofiltration. *J Membr. Sci.* 191: 109–128.
[5] Wiley, D., Fletcher, D. 2003. Techniques for Computational Fluid Dynamics Modelling of Flow in Membrane Channels. *J Membr. Sci.* 211: 127–137.
[6] Flectcher, D., Wiley, D. 2004. A Computational Fluids Dynamics Study of Buoyancy Effects in Reverse Osmosis. *J Membr. Sci.* 245: 175–181.
[7] Shakaib, M., Hasani, S.M.F., Mahmood, M. 2009. CFD Modeling for Flow and Mass Transfer in Spacer-obstructed Membrane Feed Channels. *J Membr. Sci*. 326: 270–284.
[8] Ranade, V., Kumar, A. 2006. Fluid Dynamics of Spacer Filled Rectangular and Curvilinear Channels. *J Membr. Sci.* 271: 1–15.
[9] Subramani, A., Kim, S., Hoek., M. V. 2006. Pressure, Flow, and Concentration Profiles in Open and Spacer-Filled Membrane Channels. *J Membr. Sci.* 277: 7–17.
[10] Da Costa, A. R., Fane, A. G., Wiley, D. E. 1994. Spacer Characterization and Pressure Drop Modelling in Spacer-filled Channels For Ultrafiltration. *J Membr. Sci.* 87: 79–98.
[11] Ahmad, A. L., Lau, K. K., Abu Bakar, M. Z. 2005. Impact of Different Spacer Filament Geometries on Concentration Polarization Control in Narrow Membrane Channel. *J Membr. Sci.* 262: 138–152.
[12] Saeed, A., Vuthaluru, A., Yang, Y., Vuthaluru, H.B. 2012. Effect of Feed Spacer Arrangement on Flow Dynamics Through Spacer Filled Membranes. *Desalination*. 285: 163–169.
[13] Schock, G., Miquel. A. 1987. Mass Transfer and Pressure Loss in Spiral Wound Modules. *Desalination*. 64: 339–352.
[14] Li, F., Meindersma, W., De Haan, A. B., Reith, T. 2004. Experimental Validation of CFD Mass Transfer Simulations in Flat Channels with Non-woven Net Spacers. *J Membr. Sci.* 232: 19–30.
[15] Ahmad, A. L., Lau, K. K. 2006. Impact of Different Spacer Filaments Geometries on 2D Unsteady Hydrodynamics and Concentration Polarization in Spiral Wound Membrane Channel. *J Membr. Sci.* 286: 77–92.